The PISA Pre-Main Sequence accreting models.

E. Tognelli[1], P. G. Prada Moroni[1,2], S. Degl'Innocenti[1,2]

[1] Department of Physics "E. Fermi", University of Pisa, Pisa, Italy

[2] INFN – Pisa, Italy

Introduction

Clouds fragmentation provides the seeds from which future stars form. In this contest it is commonly accepted that a crucial role in stellar formation role is played by the development of an accretion disk from which stars gain a relevant part of their final mass (e.g. Voroyob & Basu 2006).

The introduction of an accretion phase during the early stages of pre-main evolution (pre-MS) is a crucial point in theoretical stellar modelling, especially if one considers that generally in standard stellar evolutionary codes the star is supposed to evolve from the early pre-MS as an already formed object. In recent works, Baraffe et al. have shown the impact of the inclusion of accretion processes into star evolution, showing that large discrepancies among non-accreting and accreting models are present.

In the poster we present some results obtained by means of our stellar evolutionary code once the disk accretion process has been considered during the early pre-MS phases. We computed a large dataset of evolutionary tracks by varying those parameters that mainly affect accreting stellar models, in order to investigate the final effect on theoretical stellar computations of young objects.

The Models

The models presented here have been calculated with the most recent version of the PROSECCO code, recently developed in Pisa from the well tested FRANEC stellar evolutionary code (see Tognelli et al. 2011, Dell'Omodarme et al. 2012, Tognelli et al. 1012). The main physical inputs of the code are: OPAL EOS06, SCVH95 EOS, OPAL opacities for log T > 4.5 and Ferguson et al. (2005) opacities for lower T, both calculated for the solar mixture by Asplund et al. (2009). Boundary conditions are obtained interpolating detailed atmosphere model tables in T_{eff}, g and Z (Castelli & Kurucz, 2003 and Brott & Hauschildt, 2005). Convection is treated within the MLT framework, adopting our solar-calibrated α_{ML} = 1.74.

The accretion process has been accounted for following the formalism described in Siess & Livio (1997), which is valid under the hypothesis of thin-disk accretion (see e.g. Hartmann et al. 1997).

With respect to non-accreting models the main differences are listed in the following:

- Mass variation: the star gains mass at a given accretion rate (dm/dt).
- Chemical composition variation: accretion of material with the composition of the original cloud (i.e. fresh deuterium, which is important for the energetic of the accreting star).
- Energy modification: accretion of matter with a given amount of internal specific energy.

The energy per second deposed inside the star (L_{dep}) by the accreted material is a fraction of the accretion luminosity (L_{acc}),

$$L_{dep} \equiv \alpha_{acc} L_{acc} \equiv \alpha_{acc} \frac{G M_\star \dot{m}}{2 R_\star}$$

where α_{acc} is a free parameter that can assume values in the interval [0, 1] (e.g., Prialnik & Livio 1985, Hartmann et al. 1997, Siess & Livio 1997, Baraffe et al. 2009, 2010).

Accreting Models

The modelling of the accretion phase depends on the adoption of several parameters. We investigated the effect on the models of the following quantities:

- The mass of the initial protostar (seed mass of the first hydrostatic core): M_{ini} = [5, 50] $M_{jupiter}$ (Larson 1969, Masunaga & Inutsuka 2000, Boyd & Whitworth 2005, Machida et al. 2010)
- Accretion rate: dm/dt = [10^{-7}, 10^{-3}] M_{sun}/yr
- Accretion type (accretion history): constant, exponential decay, burst (Vorobyov & Basu 2005, 2006, 2009, Machida et al. 2010)
- The accretion energy: α_{acc} = [0, 1]

The computations show that the main parameter that determines the luminosity and radius of a star at a given age during the accretion phase is the accretion energy, and in particular the adopted α_{acc} value. If low-α_{acc} values are used (cold accreting models), the star gains a quite small amount of energy from the accreting matter, which only marginally affects the evolution. In this case the accreting object evolves with small radii, contracting until high central temperatures are reached, and the star enters the ZAMS. The evolution after the end of the accretion phase is strongly different from the one obtained by non-accreting models (Fig. 1).

However, the computations show that if α_{acc} is larger than a critical value, $\alpha_{acc} > \alpha_{acc,crit}$ (hot accreting models), the energy gained by the star acts to counterbalance and reverse the gravitational contraction. Such models evolve expanding from the early accreting phases reaching radii and luminosities similar to those of non-accreting counterparts close to the end of the total convective phase (Hayashi track, Fig. 1). Such a critical α_{acc}-value is found to be $\alpha_{acc,crit} \approx 0.2$ (Fig.2, see also Siess & Livio 1997, Baraffe et al. 2009).

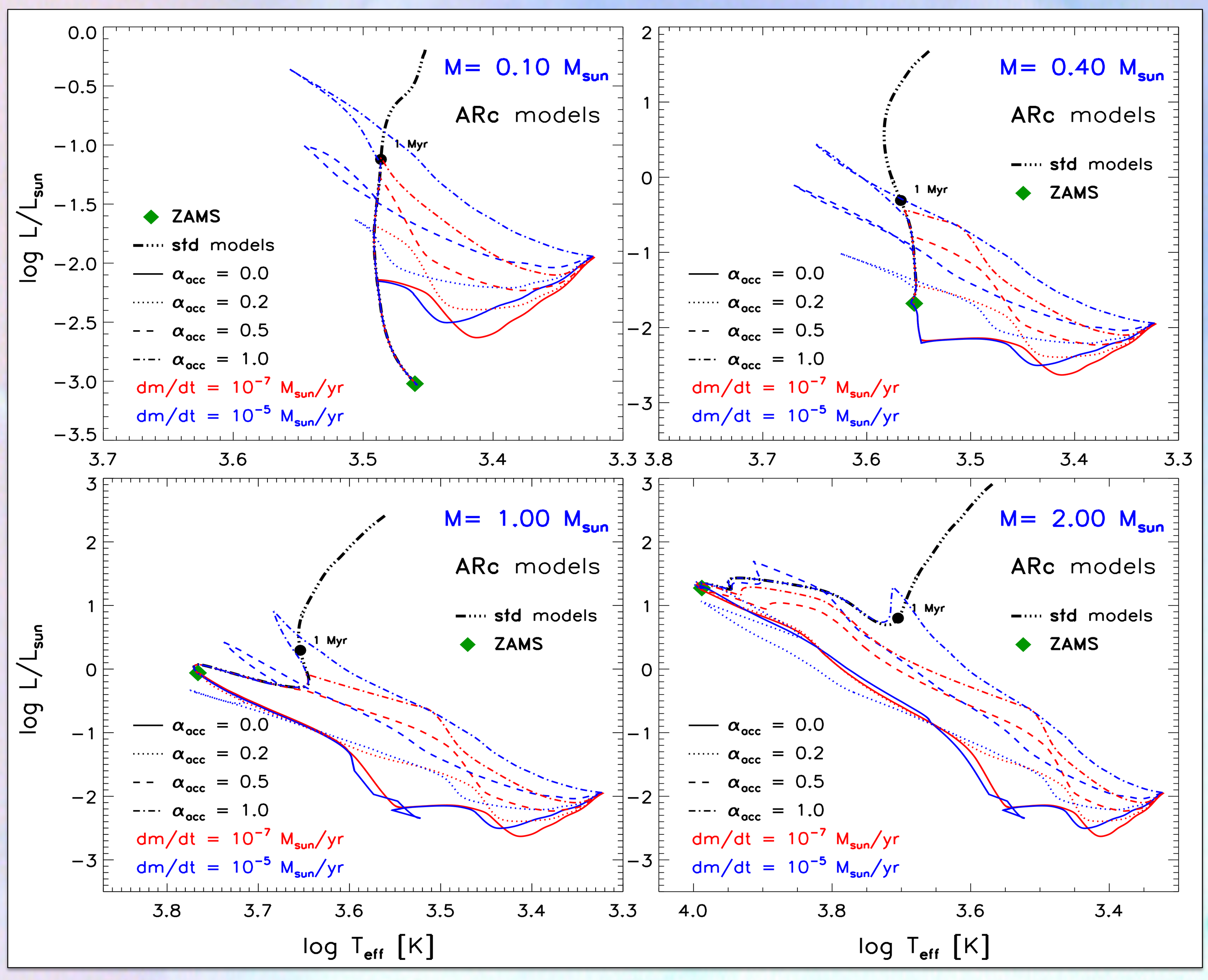

Fig. 1 Comparison between non-accreting and accreting models (with constant dm/dt) for several values of α_{acc} and for four final masses.

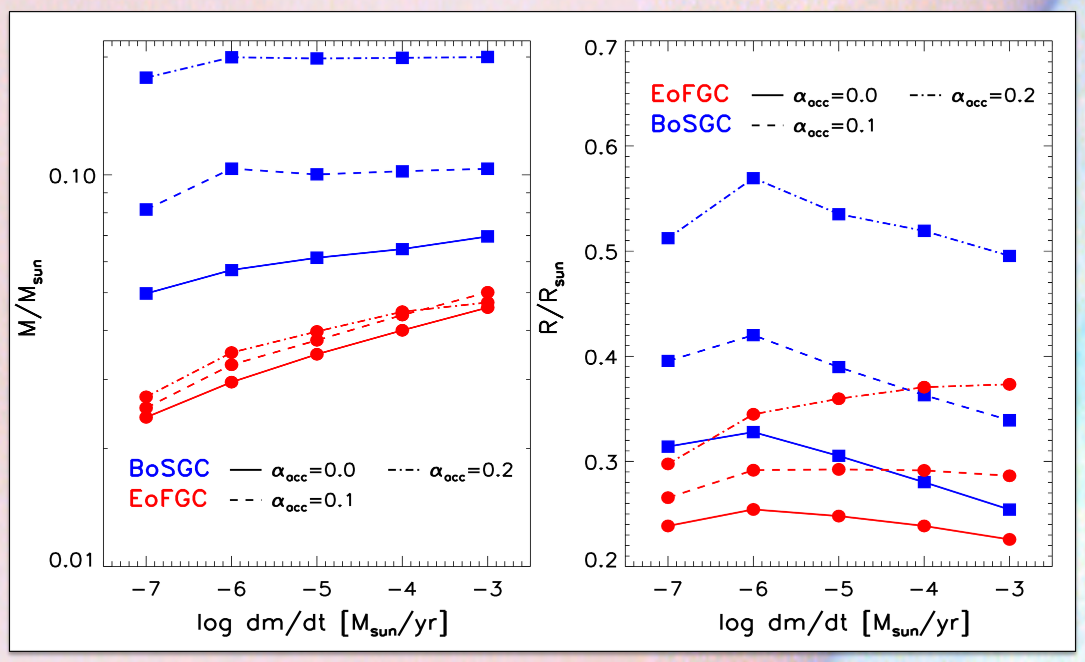

Fig. 2 Mass and radius of accreting models corresponding to the end of the first gravitational contraction (EoFGC), when the star reaches its minimum radius before the deuterium onset, and to the beginning of the second gravitational contraction (BoSGC), that is at the end of the expansion due to the d-burning. Models for several values of α_{acc} and dm/dt are shown.

Comparison with data in the HR diagram

It is worth to check the ability of accretion models to reproduce the observations and in particular the positions of young stars in the HR Diagram. Figure 3 shows the position in the HR diagram of a few available data of young objects in several associations/clusters, compared to the predictions of standard tracks (i.e. without accretion), and to the maximum region of the HR diagram that can be populated by accreting models, by varying the parameters discussed above. This simple comparison shows that, in the scenario of thin-disk accretion, cold accreting models fail in reproducing data for M > 0.1 M_{sun}. Hot accretion models (i.e. α_{acc} > 0.2 - 0.5 at least during the burst or high accretion rate phases) are required to populate the region corresponding to bright and expanse structures, where observational data lie.

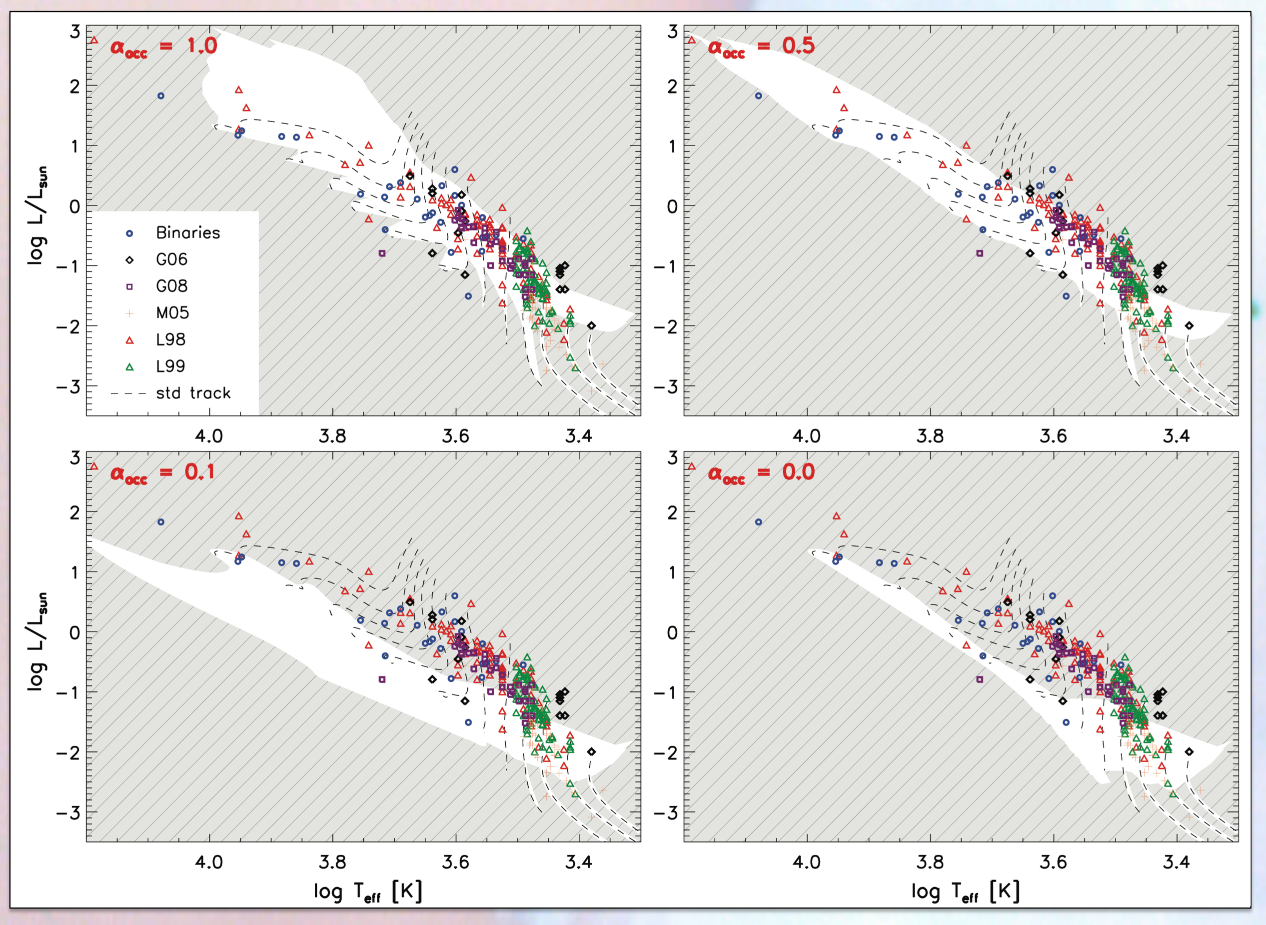

Fig. 3 The white area represents the maximum region that can be populated by accreting models by varying the seed mass, accretion rate, and accretion type, in the case of hot (top panels) and cold accretion models (bottom panels). Standard non-accreting tracks and observational data for single stars in young clusters/associations, and few pre-MS binary systems are also shown.

Surface ^{7}Li abundances

Theoretical predictions of surface ^{7}Li abundances are strongly sensitive on the choice of α_{acc}. It is interesting to notice the large depletion predicted in those cases corresponding to cold accretion models (almost independently of the adopted dm/dt or M_{ini}), where even stars of about 1.0 M_{sun} destroy almost all their lithium content within few Myr. This result strongly conflicts with lithium data in young open clusters (i.e. age < 150 – 200 Myr), where stars more massive than about 0.9 – 1.0 M_{sun} preserve their initial lithium content. This result is hint about the inability of cold accretion models to reproduce available observational data.

We also mention that the choice of different accretion rates and/or accretion history is a simple way to introduce a dispersion on the predicted lithium abundances among stars with the same mass, effective temperature and age (Fig. 4, see also Baraffe et al. 2010). A similar dispersion seems to be present in young open clusters: thus, it could be worth to check if the accretion models can justify, at least in part, the observed lithium dispersion, a point that is currently under analysis by our group.

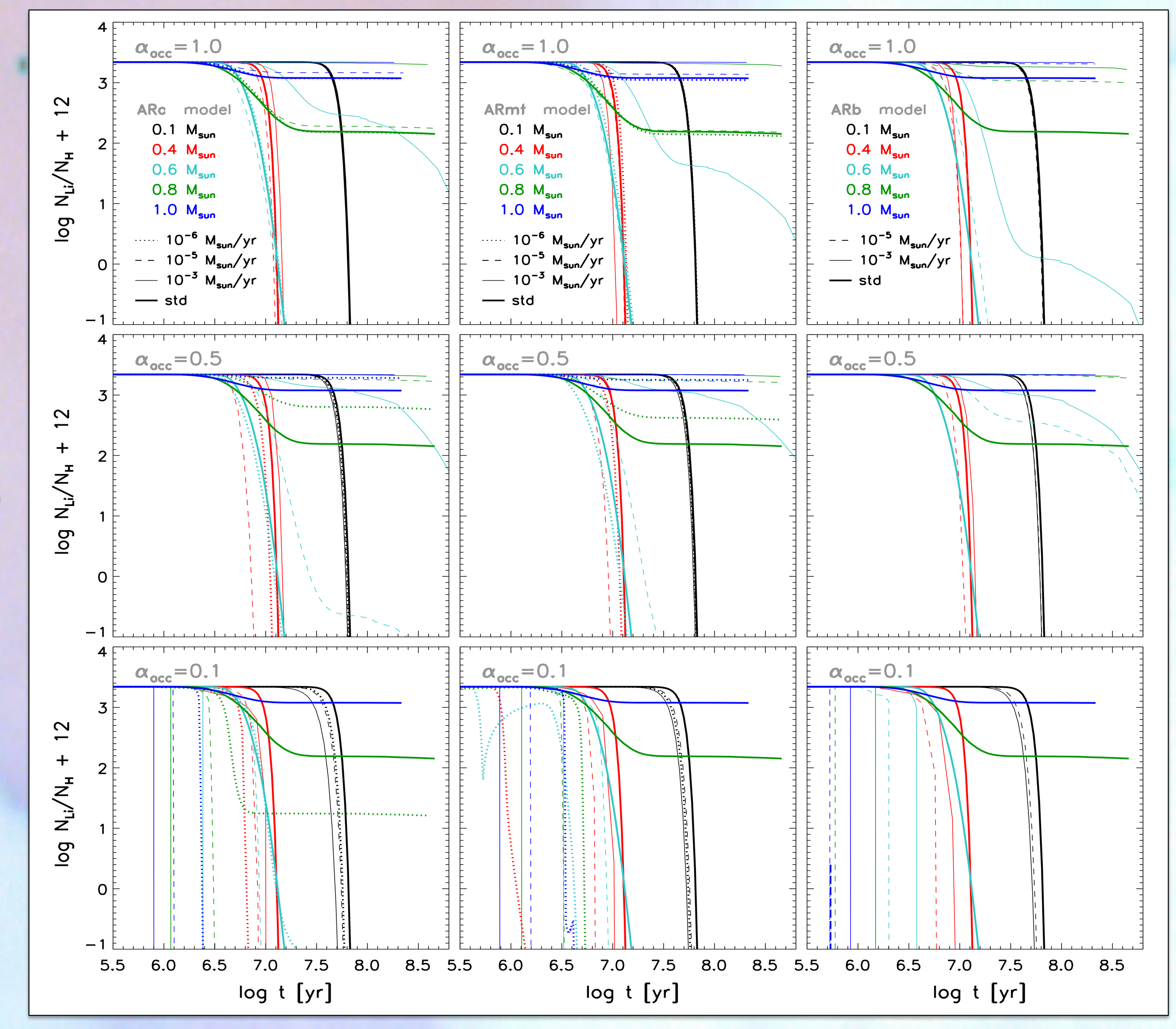

Fig. 4 Temporal evolution of the surface ^{7}Li abundance for accreting models with different masses. Constant (left panels), exponential decay (central panels), and burst (right panels) accretion types are shown. Predictions of standard non-accreting models are also shown.

References

Asplund, M. et al. (2009), ARA&A, **47**, 481
Baraffe, I., Chabrier, G., (2010), A&A, **521**, A44
Baraffe, I., Chabrier, G., Gallardo, J., (2009), ApJ, **702**, L27
Baraffe, I., Vorobyov, E.I., Chabrier, G., (2012), ApJ, **756**, 118
Boyd, D. F. A., Whitworth, A. P., (2005), A&A, **430**, 1059
Brott, I., Hauschild, P.H., (2005), ESASP, **576**, 565
Castelli, F., Kurucz, R.L., (2003), IAUS, **210**, 20
Dell'Omodarme, M. et al., (2012), A&A, **540**, A26
Ferguson J.W. et al. (2005), ApJ, **623**, 585
Hartmann, L. et al., (1997), ApJ, **475**, 770
Iglesias, C.A., Rogers, F. J., (1996), ApJ, **464**, 943 (OPAL OPACITY)
Larson, R.B., (1969), MNRAS, **145**, 271
Machida, M.N. et al., (2010), ApJ, **724**, 1006
Masunaga, H., Inutsuka, S.-i., (2000), ApJ, **531**, 350
Prialnik, D., Livio, M., (1985), MNRAS, **216**, 37
Rogers, F.J., Nayfonov, A., (2002), ApJ, **576**, 1064 (OPAL EOS)
Saumon, D., Chabrier, G., van Horn, H.M., (1995), ApJS, **99**, 713
Siess, L., Livio, M., (1997), ApJ, **490**, 785
Tognelli, E., Prada Moroni, P.G., Degl'Innocenti, S., (2011), A&A, **533**, A109
Tognelli, E., Degl'Innocenti, S., Prada Moroni, P.G., (2012), A&A, **548**, A41
Vorobyov, E.I., Basu, S., (2005), ApJ, **633**, L137
Vorobyov, E.I., Basu, S., (2006), ApJ, **650**, 956
Vorobyov, E.I., Basu, S., (2009), ApJ, **703**, 922
Vorobyov, E.I., Basu, S., (2010), ApJ, **719**, 1896